

# Numerical Modeling of QCL and Kerr Combs

Haozheng

October 8, 2025

## Abstract

This note studies the numerical modeling of quantum cascade laser (QCL) combs and Kerr combs, two prominent types of frequency combs with distinct formation mechanisms.

## Contents

|  |          |
|--|----------|
| <b>1 Concepts: Optical Frequency Combs</b> | <b>1</b> |
| <b>2 QCL Comb</b>                          | <b>4</b> |
| 2.1 Cascaded ISB Transition . . . . .      | 4        |
| 2.2 Extendon NLSE . . . . .                | 5        |
| 2.3 RF-modulated QCL Comb . . . . .        | 5        |
| <b>3 Kerr-Comb</b>                         | <b>7</b> |
| 3.1 Formation Mechanism . . . . .          | 7        |
| 3.2 Lugiato-Lefever equation . . . . .     | 8        |
| 3.3 Numerical Solution of LLE . . . . .    | 9        |

## 1 Concepts: Optical Frequency Combs

An optical frequency comb is a light source whose spectrum is constituted by a set of equidistant modes with a well-defined phase relationship between each other [1].

### Spectrum of OFCs

While located at the optical frequency region, the comb lines are fully defined by two RF frequencies: the repetition rate  $f_{\text{rep}}$  and the carrier-envelope offset frequency  $f_{\text{ceo}}$ , as illustrated in Fig. 1.  $f_{\text{rep}}$  can be directly measured using a fast photodetector, while  $f_{\text{ceo}}$  can be determined through self-referencing techniques, such as  $f$ - $2f$  interferometry for octave-spanning combs.

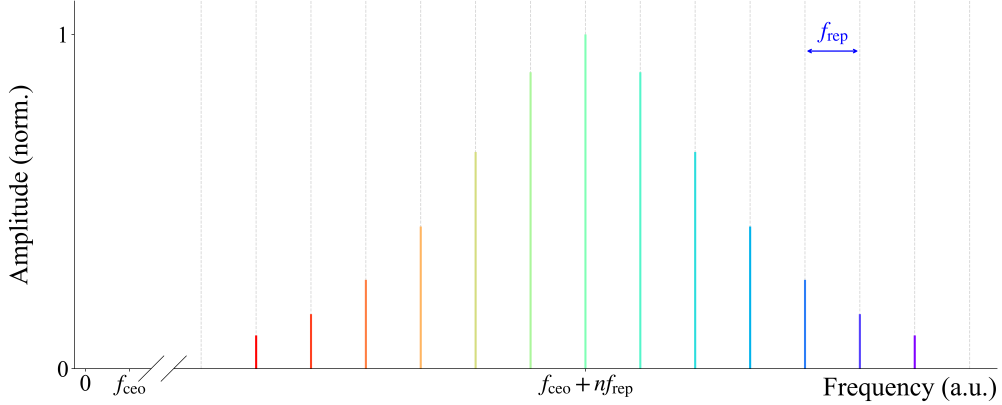


Fig. 1. Optical frequency comb spectrum.

## Fourier Analysis of OFCs

Conventionally in spectral analysis, the spectrum of Fig. 1 is written as:

$$\tilde{E}(\omega) = \sum_{n=-\infty}^{\infty} \tilde{E}_n e^{i\tilde{\phi}_n} \delta(\omega - \omega_n), \quad (1.1)$$

where  $\tilde{E}_n = \tilde{E}_{-n}$ ,  $\tilde{\phi}_n = -\tilde{\phi}_{-n}$  and  $\omega_n = 2\pi(f_{\text{ceo}} + n f_{\text{rep}}) = -\omega_{-n}$  are the amplitude, phase and frequency of the  $n$ -th comb line, respectively. The tilde denotes the frequency domain representation.

Apply the inverse Fourier transform to  $\tilde{E}(\omega)$  yields:

$$E(t) = \frac{1}{2\pi} \int_{-\infty}^{\infty} \left[ \sum_n \tilde{E}_n e^{i\tilde{\phi}_n} \delta(\omega - \omega_n) \right] e^{i\omega t} d\omega = \frac{1}{2\pi} \sum_n \tilde{E}_n e^{i\tilde{\phi}_n} e^{i\omega_n t}. \quad (1.2)$$

As a complex-valued function in time domain,  $E(t)$  can be decomposed into its amplitude and phase components:

$$E(t) \equiv E_{\text{env}}(t) e^{i\phi(t)} \quad (1.3)$$

The only consequence brought by the equidistant distribution of the comb lines is that  $E_{\text{env}}(t)$  should be periodic with a period of  $T = 1/f_{\text{rep}}$ , which can be shown by explicitly calculating  $E_{\text{env}}(t)$  from (1.2). As a result, different behaviors of the instantaneous phase  $\phi(t)$  exist in different realizations of OFCs.

## Kerr Combs: Amplitude Modulated Combs

One typical type of OFC is the Kerr comb, which can be realized by carefully detuning a microresonator with Kerr nonlinearity ( $\chi^{(3)}$ -nonlinearity) with a continuous-wave (CW) pump laser. In this case, the time-domain signal can be expressed as a baseband signal  $E_{\text{Kerr}}(t)$  modulated onto an carrier  $e^{i\omega_c t}$ :

$$E_{\text{kerr}}(t) = E_{\text{env,K}}(t) e^{i\omega_c t} \quad (1.4)$$

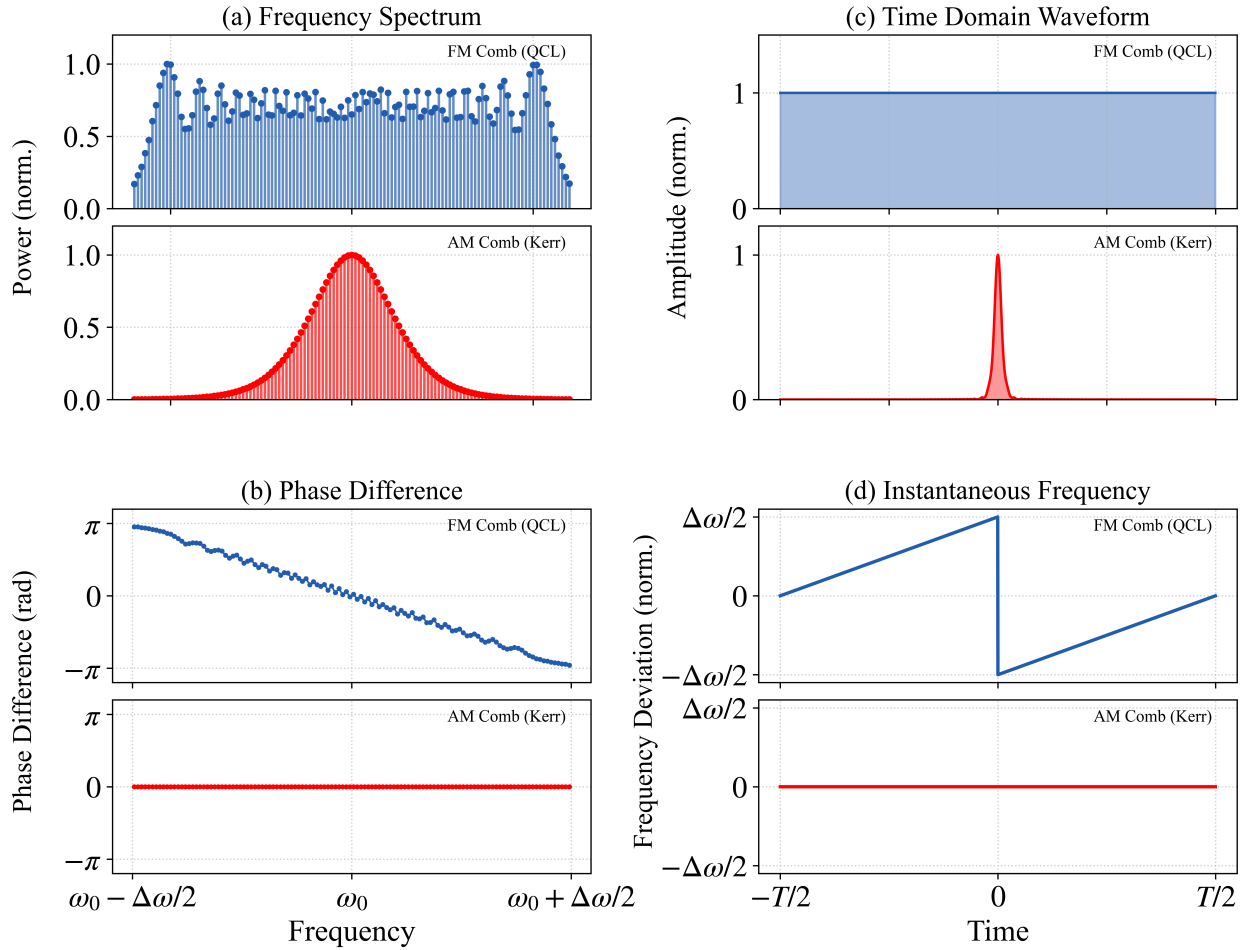


Fig. 2. Comparison of the spectral and temporal properties of AM and FM OFCs. The plots are generated from idealized models based on a forward-synthesis for the AM comb (defined in the frequency domain) and an inverse-synthesis for the FM comb (defined in the time domain). (a) The power spectra both consist of discrete lines with equal spacing. The FM comb typically has a flat-top spectral envelope, while the AM comb has a smooth,  $\text{sech}^2$ -shaped envelope. (b) The phase differences between adjacent comb lines show distinct behaviors. For the AM comb, the phase difference is **constant**, which is the condition for forming a transform-limited pulse. A **zero** constant phase difference corresponds to a pulse centered at  $t = 0$ . For the FM comb, the phase difference is **linearly varying** with frequency. (c) In the time domain, these phase relationships result in different waveforms. The AM comb forms a periodic pulse train, concentrating energy in a narrow temporal window. The FM comb, conversely, has a **nearly constant amplitude**. (d) The corresponding instantaneous frequency deviation is shown. The AM comb has a **constant instantaneous frequency** (zero deviation), which corresponds to a **linearly varying phase in time**. In contrast, the FM comb exhibits a **linearly varying instantaneous frequency** (a periodic linear chirp) within each period.

### The AM Nature of Kerr Combs

$E_{\text{env},K}(t)$  is a real-valued pulse train with a period of  $T = 1/f_{\text{rep}}$ . Its spectrum,  $\tilde{E}_{\text{env},K}(\omega)$ , is a set of equidistant discrete lines separated by  $2\pi f_{\text{rep}}$ , symmetrically centered at  $\omega = 0$ .

As suggested by the Fourier transformation, multiplying by the carrier  $e^{i\omega_c t}$  in the time domain corresponds to a shift by  $\omega_c$  in the frequency domain. Therefore,  $\tilde{E}_{\text{kerr}}(\omega)$  is a frequency-shifted version of  $\tilde{E}_{\text{env},K}(\omega)$ , now centered at the carrier frequency  $\omega_c$ .

This process is an amplitude modulation (AM) of the baseband signal, thus Kerr combs are also called AM combs. The frequencies of the individual comb lines,  $f_n$ , are described by the equation  $f_n = n \cdot f_{\text{rep}} + f_{\text{ceo}}$ , where  $f_{\text{ceo}}$  represents the offset of the entire comb grid from a perfect harmonic series, and is generally not zero.

### QCL Combs: Frequency Modulated Combs

Another typical type of OFC is the QCL comb, which can be realized by a Fabry-Pérot (FP) cavity with a gain medium possessing a fast gain recovery time (at ps scale), such as quantum cascade lasers (FP QCLs). In this case, the time-domain signal can be expressed as a constant amplitude  $E_0$  modulated by an non-trivial instantaneous phase  $\phi_{\text{QCL}}(t)$ :

$$E_{\text{QCL}}(t) = E_0 e^{i\phi_{\text{QCL}}(t)} \quad (1.5)$$

The non-trivial  $\phi_{\text{QCL}}(t)$  introduces a monotonous frequency chirp within each period, thus gaining the name of frequency modulated (FM) combs.

A schematic comparison of the AM and FM combs is shown in [Fig. 2](#).

## 2 QCL Comb

The unique properties of QCL combs originate from their gain medium, which relies on a sequence of cascaded intersubband (ISB) transitions within a semiconductor heterostructure. The fundamental process, illustrated in [Fig. 3](#), occurs in each period of this structure, which functions as an engineered three-level laser system under a DC bias.

### 2.1 Cascaded ISB Transition

An electron is injected via tunneling into the upper laser level ( $E_3$ ). It then undergoes a radiative ISB transition to the lower laser level ( $E_2$ ), emitting a photon of energy  $\hbar\omega = E_3 - E_2$ . Population inversion ( $N_3 > N_2$ ) is maintained by engineering the state lifetimes such that  $\tau_3 \gg \tau_2$ . This is achieved by rapidly depopulating the state  $E_2$  to an extraction level  $E_1$  via fast non-radiative processes. The electron then tunnels to the next stage to “cascade” the process, allowing one electron to generate many photons.

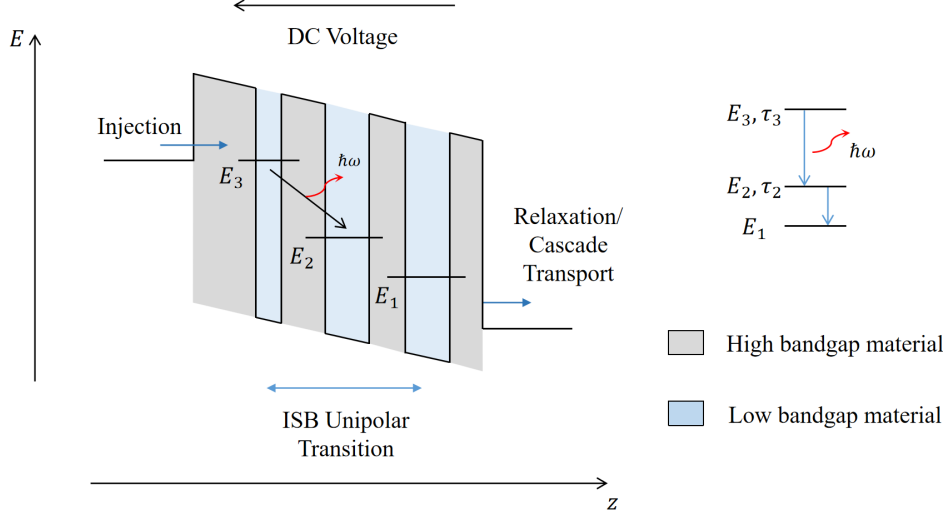


Fig. 3. ISB three-level system in a superlattice, engineered lifetimes that satisfy  $\tau_3 \gg \tau_2$  is the key to population inversion.

This entire ultrafast dynamic ( $\sim$ ps scale) is the origin of the fast gain recovery time characteristic of QCLs. This is the key physical mechanism that suppresses amplitude modulation, favoring the constant-intensity, frequency-modulated (FM) comb state.

## 2.2 Extendon NLSE

Primarily, FM combs are often simulated with Maxwell-Bloch formalisms, which lead to a series of coupled PDEs. Simultaneously, a nonlinear Schrödinger equation (NLSE) with a phase-dependent potential was derived in [2], which serves as a more intuitive model for understanding the QCL comb dynamics. This NLSE, sometimes referred to as the *extendon NLSE*, is expressed as:

$$-i\partial_T F = \frac{\beta}{2}\partial_z^2 F + \underbrace{\gamma|F|^2(\phi - \langle\phi\rangle)}_{V(F)} F + ir(|F|^2 - P_0)F \quad (2.1)$$

with  $F$  being the normalized electric field,  $T$  the slow time variable,  $\beta$  the dispersion,  $\phi$  the instantaneous phase,  $r$  the energy relaxation, and  $z$  the fast time variable.

$|F|$  is nearly constant in FM QCLs. Therefore, the potential  $\gamma|F|^2(\phi(\tau) - \langle\phi\rangle)F$  is primarily dependent on the phase of the field. Concurrently, the non-Hermitian term  $ir(|F|^2 - P_0)F$  stabilizes the field's intensity around the steady-state value  $P_0$ .

## 2.3 RF-modulated QCL Comb

The solution of (2.1) aligns well with experimental observations of free-running FM QCLs, as demonstrated in [2]. However, for stabilization and tuning purposes, QCLs are sometimes modulated with a frequency close to their mode-spacing, hence located in the RF regime. This modulation

introduces an additional potential term , which can be incorporated into (2.1) as:

$$-i\partial_T F = \frac{\beta}{2}\partial_z^2 F + \underbrace{\gamma|F|^2(\phi - \langle\phi\rangle)}_{V_{\text{SHB}}(F)} F - \underbrace{M \cos(Kz - \Delta\Omega T)}_{V_{\text{RF}}(F)} F + ir(|F|^2 - P_0)F \quad (2.2)$$

with  $M$  being the modulation depth,  $K$  the modulation wavenumber, and  $\Delta\Omega$  the detuning between the modulation frequency and the cavity round-trip frequency.

The analytical solution of (2.2) is elegantly derived in [3], together with explicit expressions of the spectrum bandwidth and the phase of the time domain signal.

With the aid of these results, a power spectrum density map with different RF detuning can be calculated, as shown in Fig. 5. Such simulations is benificial for the design of broadband, tunable, and stable frequency combs [4].

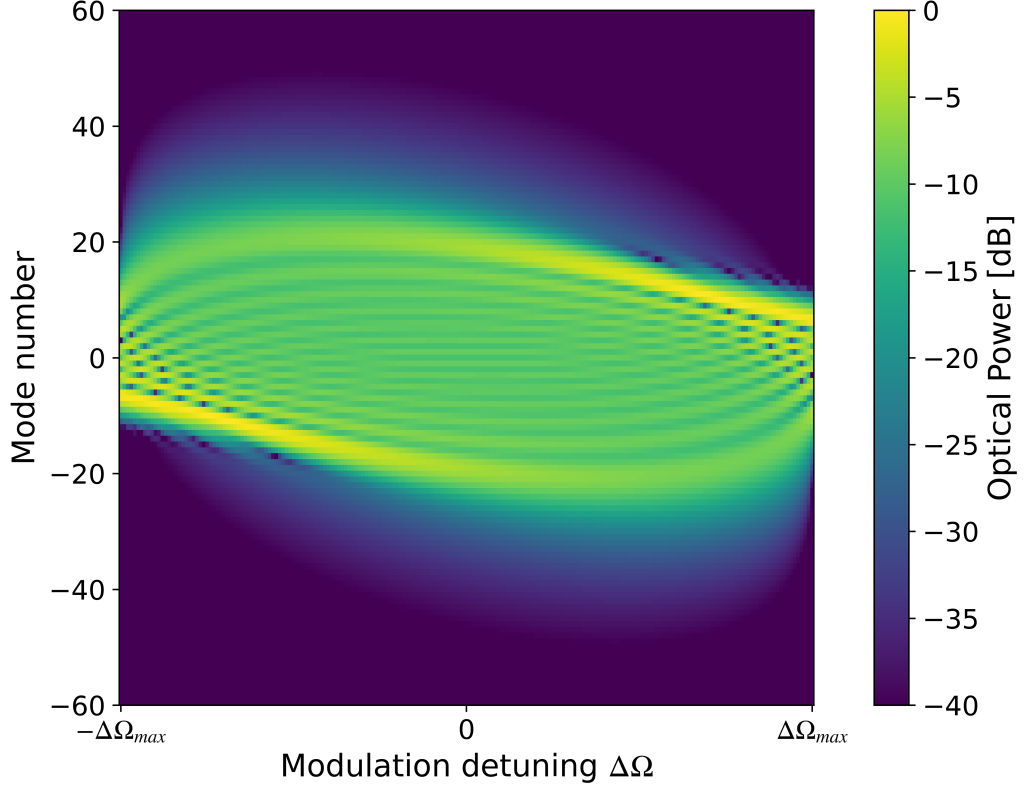


Fig. 4. 2D spectral map as a function of the modulation detuning and frequency. Codes for calculating this map are available at my [GitHub repository](#).

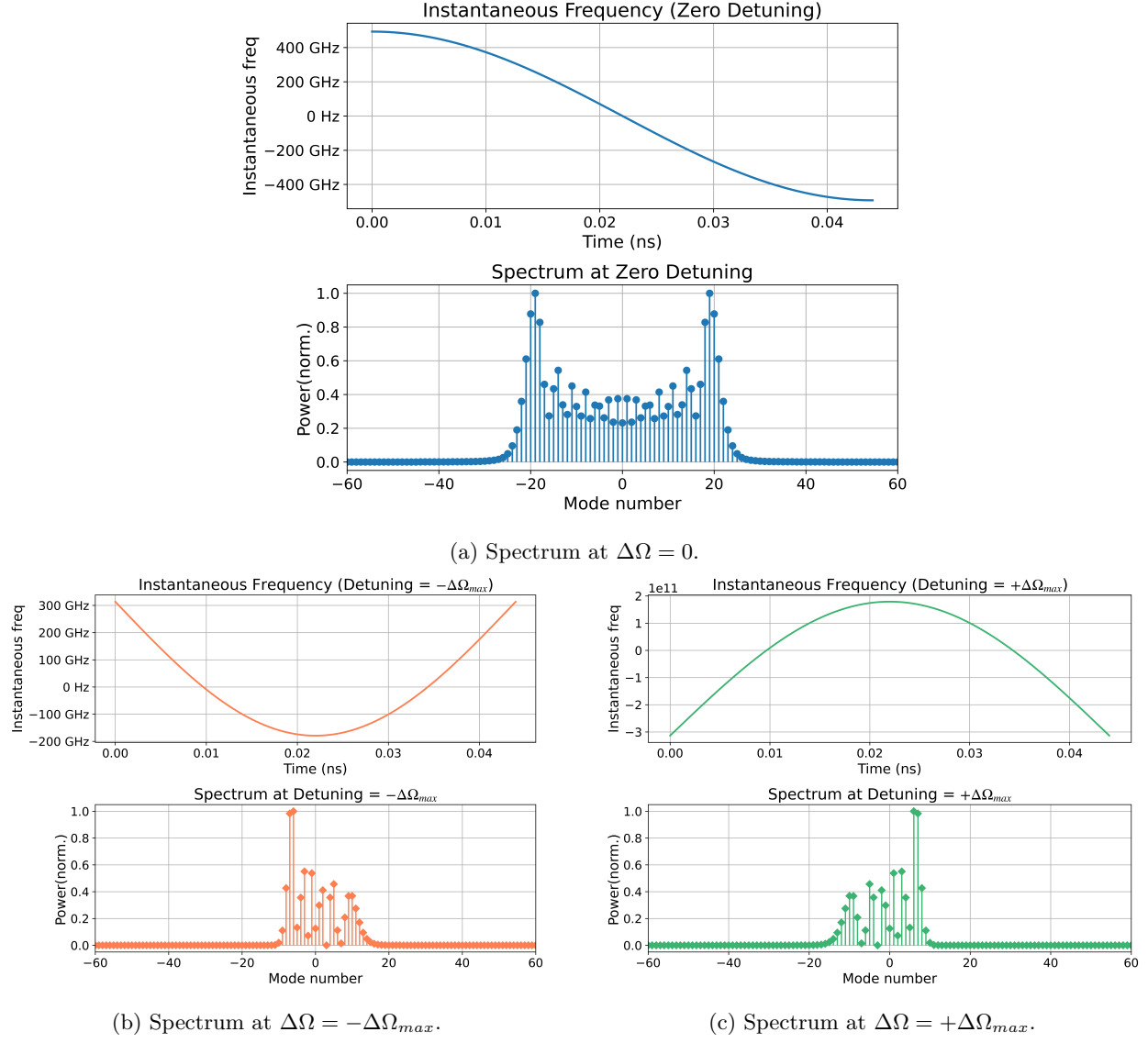


Fig. 5. Spectra of the modulation-induced frequency combs at different detunings.

### 3 Kerr-Comb

#### 3.1 Formation Mechanism

As AM combs, the key process in the formation of Kerr combs is the amplitude modulation induced by the Kerr nonlinearity. The formation mechanism can be summarized as follows [5]:

**Stage1** First, when the parametric gain overcomes the loss of the cavity, primary comb lines are generated symmetrically around the pump frequency via degenerate four-wave mixing (DWM), as shown in 6a. In this stage, dispersion  $D_2$ , nonlinear mode shift (self-phase modulation SPM and cross-phase modulation XPM) and the detuning compensate each other. FWM serves as a source of new frequencies, while only comb lines *near* the cold cavity resonances can build up.

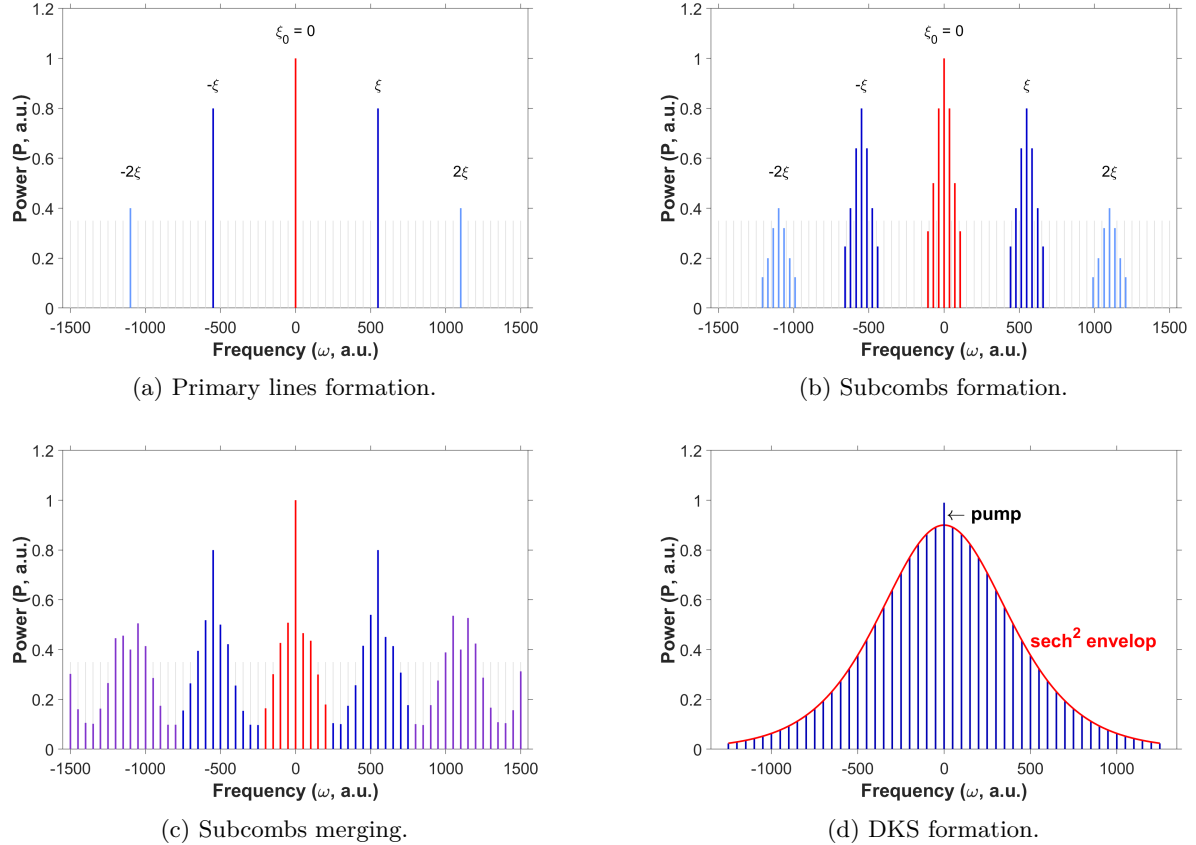


Fig. 6. Schematic of the DKS formation.

**Stage2** With reduced detuning and increased intracavity power, secondary comb lines (subcombs) are generated around the primary lines via degenerate and non-degenerate FWM with a spacing  $\delta \approx 2\pi\text{FSR}$ , as shown in 6b.

**Stage3** The spectrally separated subcombs initiated in these processes grow through non-degenerate FWM when the power coupled to the cavity is increased further, and eventually merge to form a gap-free spectrum of lines, as shown in 6c.

**Stage4** At the end of stage3, a fully filled Kerr-comb is formed, as shown in 6d.

### 3.2 Luglato-Lefever equation

Both the formation of *spatial* and *temporal* Kerr combs in microrecavities can be described by the Luglato-Lefever Equation (LLE), an equation that captures the balance between dispersion, nonlinearity, driving, and dissipation in the system, but except the thermal effects [6]. A dimensionless form of

the LLE for temporal DKS is given by <sup>1</sup> :

$$\partial_\tau \Psi = \left[ -(1 + i\zeta_0) + \frac{i}{2} \partial_\theta^2 + i|\Psi|^2 \right] \Psi + f \quad (3.1)$$

Here,  $\Psi(\tau, \theta)$  is the waveform,  $\tau$  is the normalized slow time,  $\theta$  is dimensionless longitudinal coordinate (also called fast time),  $\zeta_0$  is the dimensionless detuning , and  $f$  is the dimensionless pump power.

### 3.3 Numerical Solution of LLE

Below are numerical solutions of (3.1) using the open-source library **PyCOPe**. The figures show numerical simulations of the LLE, illustrating the intracavity field dynamics as the dimensionless detuning  $\zeta_0$ , which can be understood as the frequency difference between the cold cavity resonance and the pump laser, is swept from negative (blue-detuned) to positive (red-detuned) values. In Fig. 7, the simulation starts with a stable continuous-wave (CW) state for blue-detuned pumping ( $\zeta_0 < 0$ ).

As pump laser frequency is decreased,  $\zeta_0$  turns positive, and the intracavity state becomes unstable via modulation instability, giving rise to periodic Turing patterns in the fast time  $\theta$ . This corresponds to the initial generation of primary comb lines. A further increase in  $\zeta_0$  drives the system into a chaotic state with a highly irregular waveform and a noisy, broad spectrum.

As the pump-cavity detuning is swept into the red-detuned region ( $\zeta_0 > 0$ ), as shown in Fig. 8, the chaotic state converges to a stable dissipative Kerr soliton (DKS). This state is characterized by a localized, high-intensity pulse in the time domain and a coherent, broadband spectrum with a characteristic  $\text{sech}^2$  envelope. This soliton is the desired state for a fully coherent frequency comb. If the magnitude of the positive  $\zeta_0$  is increased too much, the pump  $f$  is no longer sufficient to sustain the soliton, which decays, and the system returns to the trivial CW solution.

---

<sup>1</sup>(3.1) is derived from eq.(8) in the supplementary material of [7].

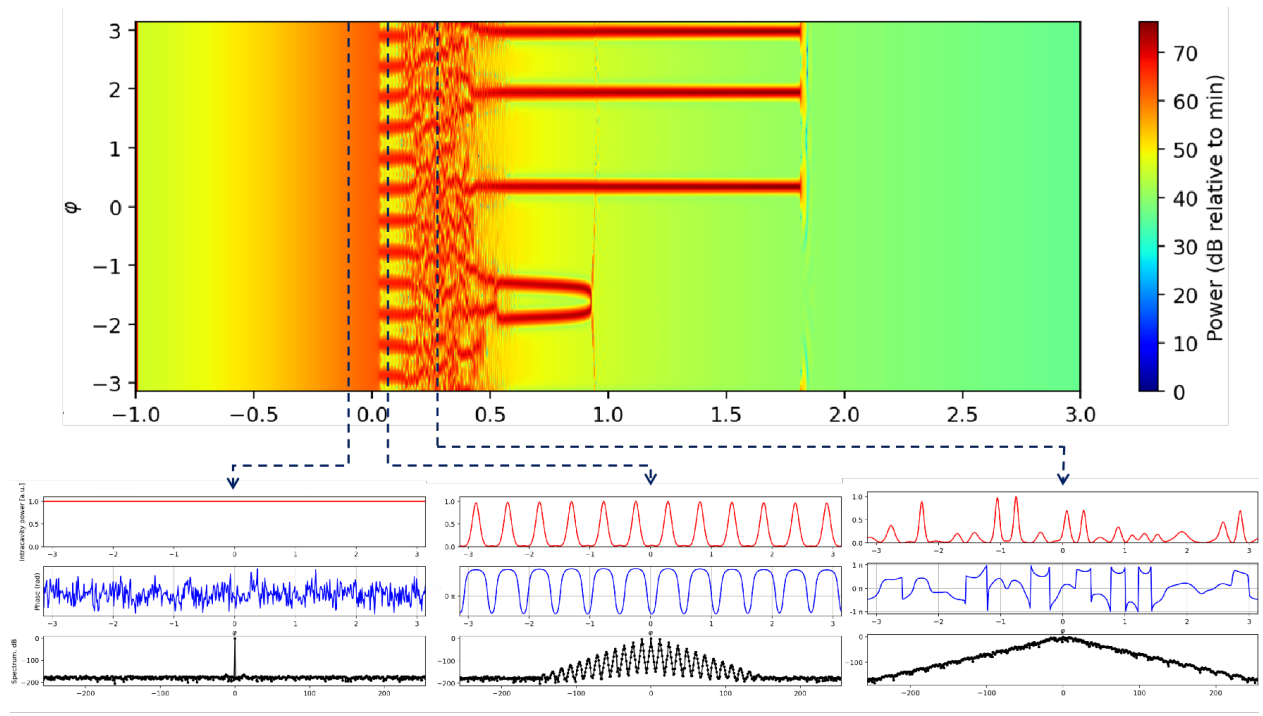


Fig. 7. CW state in the blue detuning region, Turing, and Chaos states.

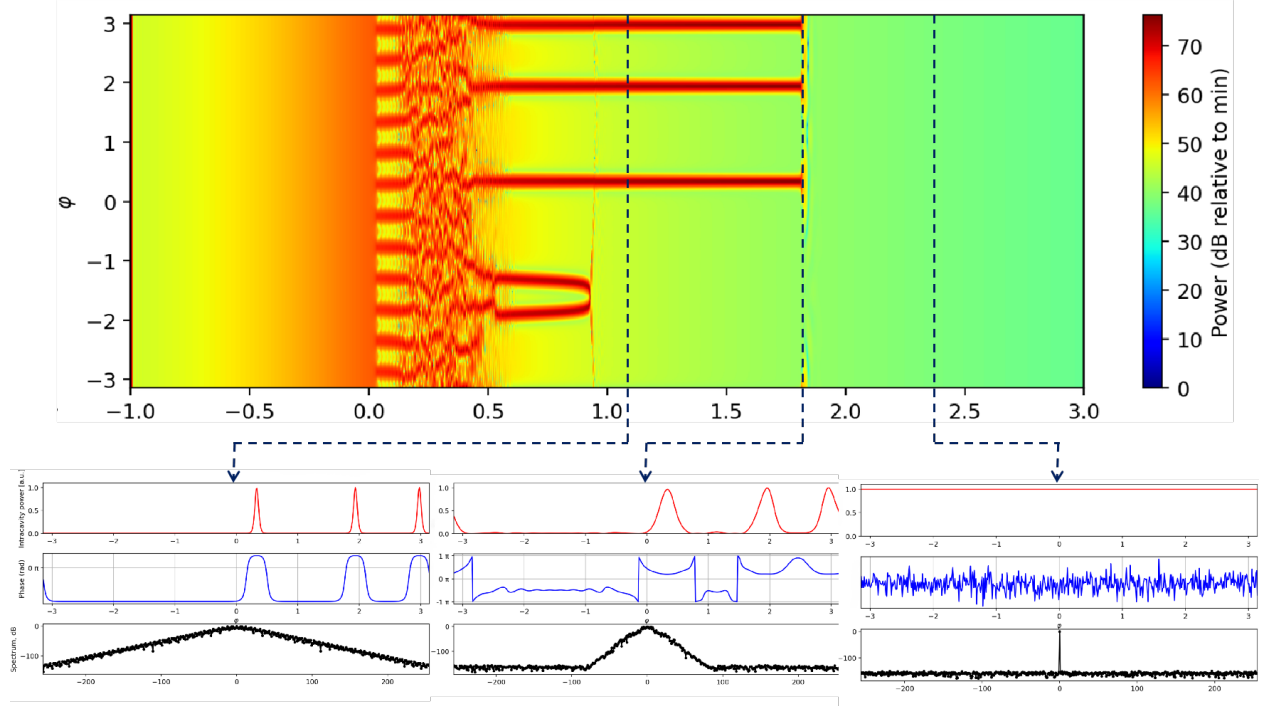


Fig. 8. Solitons, Deteriorative Solitons, and CW state in the red detuning region.

## References

- [1] Jérôme Faist, Gustavo Villares, Giacomo Scalari, Markus Rösch, Christopher Bonzon, Andreas Hugi, and Mattias Beck. Quantum cascade laser frequency combs. *Nanophotonics*, 5(2):272–291, 2016.
- [2] David Burghoff. Unraveling the origin of frequency modulated combs using active cavity mean-field theory. *Optica*, 7(12):1781–1787, Dec 2020.
- [3] Barbara Schneider. *RF-Modulation and Time-Domain Analysis of Quantum Cascade Laser Frequency Combs*. PhD thesis, ETH Zurich, 2025.
- [4] Ina Heckelmann, Mathieu Bertrand, Alexander Dikopoltsev, Mattias Beck, Giacomo Scalari, and Jérôme Faist. Quantum walk comb in a fast gain laser. *Science*, 382(6669):434–438, 2023.
- [5] Tobias J. Kippenberg, Alexander L. Gaeta, Michal Lipson, and Michael L. Gorodetsky. Dissipative kerr solitons in optical microresonators. *Science*, 361(6402):eaan8083, 2018.
- [6] Hairun Guo, Maxim Karpov, Erwan Lucas, Arne Kordts, Martin HP Pfeiffer, Victor Brasch, Grigory Lihachev, Valery E Lobanov, Michael L Gorodetsky, and Tobias J Kippenberg. Universal dynamics and deterministic switching of dissipative kerr solitons in optical microresonators. *Nature Physics*, 13(1):94–102, 2017.
- [7] Tobias Herr, Victor Brasch, John D Jost, Christine Y Wang, Nikita M Kondratiev, Michael L Gorodetsky, and Tobias J Kippenberg. Temporal solitons in optical microresonators. *Nature Photonics*, 8(2):145–152, 2014.